UC Davis
UC Davis Previously Published Works

Title

Nonequilibrium Thermodynamics in Measuring Carbon Footprints: Disentangling Structure and Artifact in Input-Output Accounting

Permalink

https://escholarship.org/uc/item/74j985nb

Authors

Loomis, Samuel P
Cooper, Mark
Crutchfield, James P

Publication Date

2021-06-07

Peer reviewed

Nonequilibrium Thermodynamics in Measuring Carbon Footprints: Disentangling Structure and Artifact in Input-Output Accounting

Samuel P. Loomis,[1, *] Mark Cooper,[2, †] and James P. Crutchfield[1, ‡]

[1]*Complexity Sciences Center and Physics Department,
University of California at Davis, One Shields Avenue, Davis, CA 95616*

[2]*Department of Human Ecology, University of California at Davis, One Shields Avenue, Davis, CA 95616*

(Dated: June 9, 2021)

Multiregional input-output (MRIO) tables, in conjunction with Leontief analysis, are widely-used to assess the geographical distribution of carbon emissions and the economic activities that cause them. We examine Leontief analysis as a model, demonstrating commonalities with modern approaches in information theory and nonequilibrium statistical mechanics. Paralleling the physical concept of thermo-majorization, we define the concept of eco-majorization and show it is a sufficient condition to determine the directionality of embodied impact flows. Surprisingly, relatively small trade deficits and geographically heterogeneous impacts greatly increase the appearance of eco-majorization, regardless of any further content in the MRIO tables used. Our results are bolstered by a statistical analysis of null models of MRIO tables developed by the Global Trade Aggregation Project.

I. INTRODUCTION

As our planet faces environmental catastrophe of unprecedented scope, it has become necessary to address human impacts on the climate and global ecosystem through multilateral action by the world's governments. Warnings have been raised about the pitfalls of too short-sighted a response. For instance, treaties that only address pollution at the point of production may effectively outsource carbon-intensive activities from signatory nations to nonsignatories, a process known as *carbon leakage* [1, 2]. Instead, a holistic response that accounts for the multifaceted social relations driving environmental impacts is required [3–7]. Acquiring the data needed to make such holistic assessments, however, is a challenge in its own right.

Multiregional input-output (MRIO) tables provide data on the monetary transactions between national-level industries, both within a nation's borders and across them [8–12]. These can be used to construct models of the interconnected global economy. MRIO tables can be ecologically extended (called EE-MRIO tables) by adding local data on the environmental impacts that arise as byproducts of production.

Leontief analysis is a method frequently paired with EE-MRIO tables to attribute production-level impacts to the (potentially distant) activities that they support—typically consumption [1, 2, 7, 13–28]. These attributed impacts are said to be *embodied* in the consumed product. The flows of embodied impacts computed from EE-MRIO tables have been utilized in policy analysis by global and national government institutions [29–32]. Leontief analysis makes key assumptions, however, whose accuracy has been brought into question, particularly when applied to existing MRIO tables [11, 12, 33]. The following explores the *consequences* of these assumptions.

Disentangling the results of a mode of analysis from mathematical artifacts that arise from the assumptions entailed is a difficult and often overlooked practice when working with complex data. For this reason, the use of specialized null models in network science has become increasingly popular [34–39]. The null models are used to randomly generate networks with special constraints designed to replicate the structural assumptions of a dataset while otherwise reducing structural biases via random connections. Following this, we use null models specifically constructed to address the structures of EE-MRIO datasets, in conjunction with mathematical analysis to elucidate the connections between the assumptions of Leontief analysis and the embodied flows it detects.

In particular, we find that when certain reasonable conditions hold on an EE-MRIO dataset—namely, relatively small trade deficits among nations and geographically heterogeneous impact intensities—the directionality of embodied impact flows to and from extremal regions is heavily influenced by the impact intensities. Notably, the MRIO tables themselves have only a secondary effect. We

* sloomis@ucdavis.edu
† mhcooper@ucdavis.edu
‡ chaos@ucdavis.edu

call the phenomenon mediating this *eco-majorization*.

Our analysis of eco-majorization relies on the general theory of majorization and Lorenz curves [40] which have found wide application in economic and social analysis [41, 42], statistical decision theory [43, 44], and statistical physics [45–49]. Majorization and Lorenz curves are a means of characterizing the differences between two distributions without reducing those differences to a single parameter. The intuition of majorization has a natural foothold in the assumptions of Leontief analysis and EE-MRIO tables. Due to this, heterogeneities in impact intensities drive embodied flows in a manner directly analogous to physical diffusion.

Section II covers the relevant mathematics of EE-MRIO tables and Leontief analysis, the construction of our null models, and the necessary details for using majorization. Section III shows how our symmetrically-constructed null model of trade recovers asymmetric embodied flows quite regularly. To explain this, we define eco-majorization, demonstrate how it couples the impact intensities to flows of embodied resources, and explain why (under the aforementioned conditions) Leontief analysis is structurally biased towards eco-majorization. Further analysis of the null model shows that relaxing our conditions mitigates majorization's effects. Section IV closes discussing the implications of these results for analyzing EE-MRIO tables and environmental accounting.

II. BACKGROUND AND METHODS

A. Input-output analysis

The following describes the basic components of EE-MRIO analysis, focusing on aspects relevant to the developments in Sec. III. Useful reviews of input-output methods are found in Refs. [11, 12, 28]. Additionally, we present a somewhat more detailed description of these methods in App. A.

A MRIO table consists of a set of regions $\mathcal{R}$ and a set of industrial sectors $\mathcal{I}$. The full global set of sectors is given by $\mathcal{R} \times \mathcal{I}$, with pair $(r, i) \in \mathcal{R} \times \mathcal{I}$ corresponding to industry i in region r. An input-output table over these industries is characterized by three pieces: the *value-added* block-vector v_{ri}, describing the incomes paid by industry i to labor, land, and capital in the region r; the *demand* block vector d_{ri}, describing the value purchased from industry i by private or government spending and investment; and the inter-industrial block matrix $Z_{ri,sj}$ that describes the flow of money from industry j in region s to industry i in region r. These quantities are assumed to be measured over a fixed time interval.
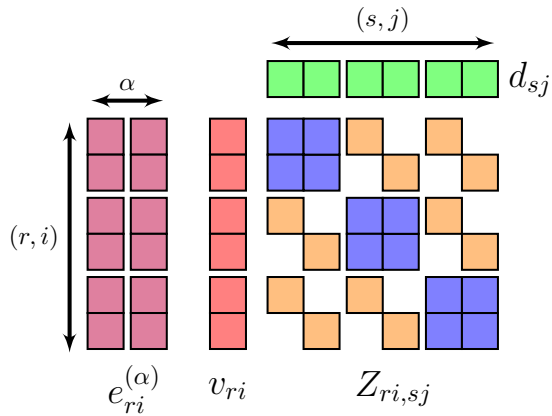

FIG. 1. Block-matrix structure of a typical EE-MRIO table with $|\mathcal{I}| = 2$ and $|\mathcal{R}| = 3$. Blue and orange blocks are arranged into the single block-matrix $Z_{ri,sj}$, representing the value of all inter-industry transactions. Red blocks correspond to the value-added vector v_{ri}, consisting of all returns to wages, profits, and rent. And, the green blocks correspond to the final demand vector d_{ri}, consisting of all expenditures by consumers, governments, and investors. Pink blocks represent two separate ecological impact distributions $e_{ri}^{(\alpha)}$.

In a block matrix each row and column indicates a pair (r, i), so that the first $|\mathcal{I}|$ indices correspond to all the industries in one region, and so on; Fig. 1 gives a visual aid. Additionally, simplifying constructs are often used in collecting and apportioning the data. For instance, in the dataset GTAP 8 (discussed shortly), $\mathcal{I}$ contains a duplicate of each industry, one for managing imports and the other for domestic industries. Cross-regional trade from r to s can only go from the domestic copy of industry i in r to the import copy of industry i in s. That is, cross-regional trade is not treated as cross-industry. This is represented visually by the diagonal structure of off-diagonal blocks in Fig. 1.

MRIO table components are constrained by the following identity which demands all accounts balance. That is, for each industry, all money outlaid on materials and incomes equals the total value of output purchased. The total throughput is denoted by the block-vector z_{ri}:

$$z_{ri} := \underbrace{v_{ri} + \sum_{s,j} Z_{sj,ri}}_{\text{Outlays}}$$
$$= \underbrace{\sum_{sj} Z_{ri,sj} + d_{ri}}_{\text{Outputs}} \ . \quad (1)$$

A consequence is that global income $y := \sum_{ri} v_{ri}$ and global spending $\sum_{ri} d_{ri}$ are equal. Whereas, *regional* income $\hat{y}_r := \sum_i v_{ri}$ and spending $\hat{x}_r := \sum_i d_{ri}$ are *not* necessarily equal. We refer to their difference $\hat{x}_r - \hat{y}_r$ as

the *regional deficit.*

The technical coefficients $C_{ri,sj} := Z_{ri,sj}/z_{sj}$ express what proportion of outlays are committed to specific industries. Clearly, $Z_{ri,sj} = z_{sj}C_{ri,sj}$. Given this, the balance identity Eq. (1) may be expressed as a linear-algebraic equation $\mathbf{z} = \mathbf{Cz} + \mathbf{d}$, with matrix multiplication between block-matrix $\mathbf{C}$ and block-vector $\mathbf{z}$. The solution is given by:

$$\mathbf{z} = (\mathbf{I} - \mathbf{C})^{-1}\mathbf{d} , \qquad (2)$$

where $\mathbf{I}$ is the identity matrix and one uses the matrix inverse. Written more explicitly, we have:

$$z_{ri} = \sum_{sj} \left[(\mathbf{I} - \mathbf{C})^{-1}\right]_{ri,sj} d_{sj} . \qquad (3)$$

This expresses the total output as a column-sum of the matrix $(\mathbf{I} - \mathbf{C})^{-1}\mathbf{D}$. The sum allows us to break sector i's total output into parts, each attributed to a particular final region of demand s. The proportions of this decomposition are given by the attribution matrix $\mathbf{A}$:

$$A_{ri,s} := \frac{\sum_j \left[(\mathbf{I} - \mathbf{C})^{-1}\right]_{ri,sj} d_{sj}}{z_{ri}} , \qquad (4)$$

which characterizes what portion of the throughput of sector (r, i) originated as demand in region s. Determining these attributions is called *Leontief analysis* after its originator [8, 9].[1]

The application of Leontief analysis which occupies us is its use in attributing the *ecological impacts* of particular industries to the parties whose demand stimulates the impact. This is accomplished through the augmentation of an MRIO table with *environmental extensions.* These are a series of block-vectors $e_{ri}^{(\alpha)}$ (the series being indexed by α) each of which characterizes what quantity of ecological impact α may be directly attributed to the industry i in region r. For instance, if α is CO_2, then $e_{ri}^{(\alpha)}$ is the total megatons of CO_2 released by the activity in sector (r, i). If α is labor-time, then $e_{ri}^{(\alpha)}$ is the amount of human-hours utilized by sector (r, i).

We denote the *regional direct impact* by $\hat{e}_r^{(\alpha)} := \sum_i e_{ri}^{(\alpha)}$ and the *total impact* by $E^{(\alpha)} := \sum_r \hat{e}_r^{(\alpha)}$. Using the attribution matrix, we then define the *attributed impact*

---

[1] The analysis may be reversed to attribute outputs to factors $\mathcal{Y}$ rather than to final demands $\mathcal{D}$. While not explicitly considered here, the results derived for demand-based accounting apply symmetrically to factor-based accounting.

vector as:

$$\hat{a}_s := \sum_{ri} e_{ri}^{(\alpha)} A_{ri,s} . \qquad (5)$$

This, in theory, characterizes the quantity of impact α for which the demand in region s is responsible.

The utility of Leontief analysis rests on two main assumptions [12]:

(L-1) Sectors produce homogeneous products: Due to this, we do not reweight the technical coefficients to reflect differences between the purchasing sectors—they purchase the same item.

(L-2) Sectoral products are homogeneously priced: Every buyer pays the same unit price. This again allows using the technical coefficients without modification to reflect differences in the inputs required per dollar for different purchasers.

We return to the assumptions later to discuss their impact on the results of Leontief analysis.

For now, we mention two important reflections of these assumptions in the results above. First is the fact that $\sum_s A_{ri,s} = 1$ for all regions r and industries i. This gives $A_{ri,s}$ the property of stochasticity. That the direct impacts and attributed impacts can be related by a single stochastic matrix is a reflection of the homogeneity in each of these assumptions.

Second, income itself can be treated as an impact. The value-added vector, when passed through the attribution matrix, returns the regional spending vector:

$$\hat{x}_s = \sum_{ri} v_{ri} A_{ri,s} , \qquad (6)$$

While App. A explains the identity's mathematical origin, conceptually it arises from assumption (L-2): Impacts are attributed to demand in the exact same manner that incomes are attributed to spending. Both the stochasticity of $A_{ri,s}$ and Eq. (6) will be critically important when applying majorization.

Finally, we define several miscellaneous terms that feature in our analysis. Given impact α, we define the α-*intensity* $f_{ri}^{(\alpha)}$ of sector (r, i) as the ratio of environmental impact to economic impact. For instance, for CO_2 this represents the pollution released for each dollar of activity in sector (r, i). The most intuitive interpretation is seen in the case of labor-time, where the intensity is a kind of inverse wage.

While there are many different precise definitions of intensity, for our needs we define it for sectors and regions

as:

$$f_{ri}^{(\alpha)} := \frac{e_{ri}^{(\alpha)}/v_{ri}}{E^{(\alpha)}/Y} \;, \quad \hat{f}_r^{(\alpha)} := \frac{\hat{e}_r^{(\alpha)}/\hat{y}_r}{E^{(\alpha)}/Y}$$

That is, we take the ratio of the impact $e_{ri}^{(\alpha)}$ to the *value-added* v_{ri} by sector (r,i). This directly relates the emission at a given stage of production to the value added to the region by that production. (Not counted in this is the economic input from other industries, as this value has already been counted as value-added in another industry.) To remove dependence on the units used, we normalize the ratio using the ratio of totals.

Embodied flows resulting from Leontief analysis are frequently quantified by one or both of the following proxy measures [7, 15, 17, 19–21, 23–27]:

1. The net exports $\boldsymbol{\xi}^{(\alpha)} = (\xi_r^{(\alpha)})$ of attributed impact, as a share of total global impact:

$$\xi_r^{(\alpha)} = \frac{\hat{e}_r^{(\alpha)} - \hat{a}_r^{(\alpha)}}{\sum_r \hat{e}_r^{(\alpha)}} \;.$$

2. The consumption/production ratio $\boldsymbol{\rho}^{(\alpha)} = (\rho_r^{(\alpha)})$ of attributed impact to direct impact:

$$\rho_r^{(\alpha)} = \frac{\hat{a}_r^{(\alpha)}}{\hat{e}_r^{(\alpha)}} \;.$$

Naturally, these are closely related, as they ultimately express the relationship between the relative sizes of produced impacts and consumed impacts.

B. Null models and GTAP 8

Null models, also *configuration models*, are a popular tool in the study of complex networks. They are widely applied to social [34, 50], animal [38, 39], and biological [37] networks to separate-out structures detected in empirical networks from those engendered by methodological assumptions [35, 36]. Often particular aspects of the networks—such as degree distribution—are held constant while all remaining aspects are randomized.

The following constructs a null model of global trade that maintains similar technical coefficients between industries, but "social coefficients"—those determining the relations between nations, dependency on imports, proportion paid to factors, and so on—are entirely randomized. This way, structures that consistently arise from Leontief analysis of networks drawn from this model cannot be attributed to social relations. They are, rather, artifacts of the assumptions of Leontief analysis.

The Global Trade Aggregation Project (GTAP) [51] offers an extensive collection of transaction tables over a large number of regions and sectors. GTAP has been used as the EE-MRIO source data in many studies of embodied carbon emissions and other impacts [7, 17, 20, 22, 26]. We used GTAP 8 covering 134 regions (114 of which are countries), with 57 industrial sectors within each region, as well as 5 factor sectors (skilled and unskilled labor, capital, land, and natural resources), the standard 3 final demand sectors, and further sectors that fall outside the scope of our analysis. The data on these sectors was used to construct a multiregional input-output table. GTAP 8 comes directly with environmental extensions for carbon and energy use, and a number of satellite datasets exist providing further extensions. As an additional point of comparison, we used the satellite GMig2 [52] that provides information on labor inputs in human-years.

The carbon and labor data provided by GTAP 8 and GMig2 allowed us to compute the carbon and labor intensities, $\hat{\mathbf{f}}^{(\mathrm{CO_2})}$ and $\hat{\mathbf{f}}^{(\mathrm{L})}$, respectively, over 17 *megaregions* formed by aggregating the 134 GTAP standard regions.

We then constructed a null model for generating trade datasets over a reduced MRIO system with 4 factors, 16 industrial sectors, and 17 regions (aggregated from the GTAP sectors and regions). The null model has two parameters: a scalar ζ_X and a vector $\zeta_{C,i}$ taking values over industrial sectors. It makes liberal use of Dirichlet distributions as the source for drawing randomly-generated stochastic matrices from which the input-output tables are procedurally constructed.

Recall that a Dirichlet distribution $\mathrm{Dir}(\alpha_1, \ldots, \alpha_K)$ is defined on the simplex of probability vectors over K elements. The density function of $\mathrm{Dir}(\alpha_1, \ldots, \alpha_K)$ is given by:

$$d(p_1, \ldots, p_K) \propto \prod_{i=1}^{K} p_i^{\alpha_i - 1} \;.$$

Notably, when $\alpha_1, \ldots, \alpha_K$ all equal 1, the Dirichlet distribution draws from all probability vectors with equal weight (a uniform Dirichlet). Otherwise, it tends to draw probability vectors whose weight distribution is similar to that of the vector $(\alpha_1 - 1, \ldots, \alpha_K - 1)$, varying to a degree that is inversely proportional to $\alpha_0 := \sum_{i=1}^{K} \alpha_i$ (a nonuniform Dirichlet).

The null model uses nonuniform Dirichlet distributions to draw the values of the regional technical coefficients so that they are similar to the global coefficients $\tilde{C}_{ij}^{(\mathrm{GTAP})}$ from GTAP 8 with a degree of variation controlled by the parameter $\zeta_{C,i}$ for each industrial sector i. All other coefficients—which we call *social coefficients*—are constructed from combining uniform Dirichlet distributions.

Using the technical and social coefficients, we can use another nonuniform Dirichlet to generate the regional spending and income distributions so that the regional deficit is small, controlled by parameter ζ_X. Baseline values $\bar{\zeta}_{C,i}$ and $\bar{\zeta}_X$ are derived to replicate the variation among regional technical coefficients and deficits in the GTAP 8 data. The precise construction is described in Appendix B.

Additionally, we built a second, simpler null model for producing environmental extensions. It generates impact intensities, with control over the heterogeneity of intensity across regions and sectors. The imaginary resource that this impact represents is termed *unobtainium* or simply U. The null model involves constructing a new parameter ζ_U. We sample *unnormalized* intensities, denoted $\phi_{ri}^{(U)}$, as:

$$\phi_{ri}^{(U)} \sim \mathrm{Dir}(\alpha_{ri} = \zeta_U) \ .$$

ζ_U is set to a low value—our baseline is $\bar{\zeta}_U = 0.05$—resulting in the Dirichlet sampling distributions with high peakedness around randomly selected sectors and so assuring heterogeneity. By increasing ζ_U, we can reduce heterogeneity. The normalized intensities, for a given MRIO, are then determined as:

$$f_{ri}^{(U)} = \frac{\phi_{ri}^{(U)}}{\sum_{s,j} v_{sj} \phi_{sj}^{(U)}} \ .$$

Combining both null models allows generating a wide sampling of EE-MRIO tables with random social coefficients, while controlling for technical coefficients, regional deficits, and impact heterogeneity. These last two attributes, in particular, are important for majorization, as we will show.

C. Majorization and statistical mechanics

To fully appreciate the results coming from the null models, we must compare various distributions. To this end, we introduce a tool with a long tradition that recently gained traction and found significant development in information theory and statistical physics. The tool in question is *majorization*—more specifically, relative majorization [40, 42, 53]. We describe the necessary background below and also provide a primer in Fig. 2.

Given two probability distributions $\mathbf{p} = (p_i)$ and $\mathbf{q} = (q_i)$ defined over a finite set $\mathcal{S}$, we construct their *Lorenz curve* $\ell_{\mathbf{p},\mathbf{q}} : [0,1] \to [0,1]$ as the piecewise convex function

connecting the points (x_n, y_n):

$$x_n = \sum_{m=1}^{n} p_{i_m}$$
$$y_n = \sum_{m=1}^{n} q_{i_m} \ ,$$

where $(i_m) = (i_1, i_2, \dots)$ orders the set $\mathcal{S}$ so that p_{i_m}/q_{i_m} is monotonically decreasing in m.

Given two pairs of distributions $(\mathbf{p}, \mathbf{q})$ and $(\mathbf{p}', \mathbf{q}')$, if $\ell_{\mathbf{p},\mathbf{q}}(x) \geq \ell_{\mathbf{p}',\mathbf{q}'}(x)$ for all $x \in [0,1]$, then we say that $(\mathbf{p}, \mathbf{q})$ *majorizes* $(\mathbf{p}', \mathbf{q}')$ [42]:

$$(\mathbf{p}, \mathbf{q}) \succeq (\mathbf{p}', \mathbf{q}') \ .$$

An intuitive application of majorization in fact arose in its first use as an indicator of economic inequality [41]. In this context, if $\mathbf{p}$ describes the population distribution and $\mathbf{q}$ the wealth distribution, the Lorenz curve completes statements of the type "The richest $x\%$ of the population holds $\ell_{\mathbf{p},\mathbf{q}}(x)\%$ of the wealth." One country can be said to be definitively more unequal than another if its Lorenz curve is always higher. Majorization generalizes this relationship.

The connection between majorization and nonequilibrium statistical mechanics, as well as its connection to our work, arises as a consequence of the *Blackwell-Sherman-Stein* (BSS) theorem [43, 44]: $(\mathbf{p}, \mathbf{q}) \succeq (\mathbf{p}', \mathbf{q}')$ if and only if there exists a stochastic matrix $\mathbf{T}$ such that $\mathbf{Tp} = \mathbf{p}'$ and $\mathbf{Tq} = \mathbf{q}'$. This connection is profound, given the frequent appearance of stochastic matrices in statistical mechanics, information processing, stochastic processes, game theory, and decision theory, and far more.

It has quite recently found significant application in the intersection between information theory and nonequilbrium statistical mechanics. Actions taken upon a thermodynamic system can be described as stochastic matrices over a system's microstates. In this setting, it can be shown that any action (described by stochastic matrix $\mathbf{t}$) that satisfies (i) energy conservation, (ii) Liouville's theorem or information conservation, and (iii) access to a thermal reservoir of temperature T must obey the constraint:

$$\sum_j t_{i|j} \gamma_j(T) = \gamma_i(T) \ , \tag{7}$$

where γ_i is the Boltzmann-Gibbs distribution:

$$\gamma_i(T) = \frac{e^{-E_i/kT}}{Z(T)}, \quad Z(T) = \sum_i e^{-E_i/kT}$$

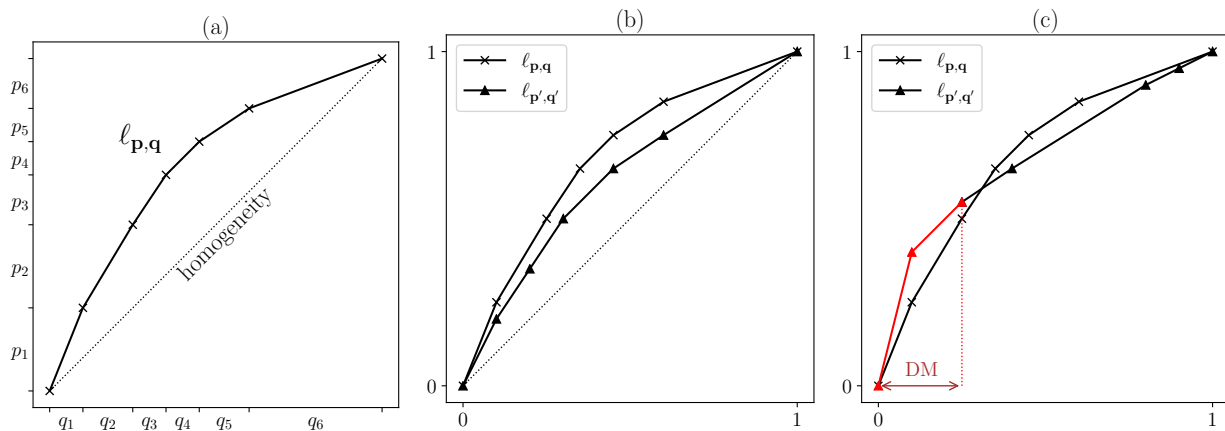and $\mathbf{E} = (E_i)$ defines the energies of each microstate i [45].

FIG. 2. Majorization Primer: *(a)* Example a Lorenz curve for a pair of distributions $(\mathbf{p}, \mathbf{q})$ over 6 elements. We assume the elements are indexed so that p_i/q_i is monotonically decreasing. $\mathbf{p}$ and $\mathbf{q}$ are not homogeneous with respect to one another, and so the Lorenz curve bows out above the diagonal. *(b)* An example of two pairs, $(\mathbf{p}, \mathbf{q})$ and $(\mathbf{p}', \mathbf{q}')$, such that $(\mathbf{p}, \mathbf{q}) \succeq (\mathbf{p}', \mathbf{q}')$. Visually, this means that the second Lorenz curve is fully beneath the first and, therefore, closer to the line of homogeneity. *(c)* Example where majorization does not hold. The extent of failure can be described by the *dismajorization*, defined as the total $\mathbf{q}'$-probability associated with the majorization-breaching vertices. "DM" stands for dismajorization.

The significance of this observation is that even when operating on a distribution $\mathbf{p}$ that is far from equilibrium—that is, *not* equal to $\boldsymbol{\gamma}(T)$—the actions we take must still satisfy Eq. (7). Using the BSS theorem, we learn that a distribution $\mathbf{p}$ can be physically transformed into another $\mathbf{p}'$ using a bath at temperature T only if $(\mathbf{p}, \boldsymbol{\gamma}(T)) \succeq (\mathbf{p}', \boldsymbol{\gamma}(T))$. It is said in this case that $\mathbf{p}$ *thermo-majorizes* $\mathbf{p}'$ [48]. This connection between majorization and thermodynamics has been used to derive a number of relations that leverage thermodynamic fluctuations to extract work in the nanoscale, single-shot regime [47–49, 53].

When majorization does not hold, it may hold approximately—a fact that can still result in many of the same consequences of majorization. It will be useful to have a quantification of dismajorization that allows us to distinguish between small and large violations of majorization.

We define the *dismajorization* $\mathrm{DM}\left[(\mathbf{p}, \mathbf{q}); (\mathbf{p}', \mathbf{q}')\right]$ of two pairs of curves in the following way. Let (i_m) be the same ordering of indices used above and let x'_n and y'_n be defined in the same manner as x_n and y_n but for the pair $(\mathbf{p}', \mathbf{q}')$. Finally, let $\mathcal{N}$ be the set of n such that $y'_n > \ell_{\mathbf{p},\mathbf{q}}(x'_n))$. Then we define:

$$\mathrm{DM}\left[(\mathbf{p}, \mathbf{q}); (\mathbf{p}', \mathbf{q}')\right] = \sum_{n \in \mathcal{N}} q'_{i_n}$$

as the total probability associated with the points where the second Lorenz curve exceeds the first.

III. RESULTS

Leontief analysis of the null-model MRIO tables paired with the empirical labor and CO_2 distributions exposed a strong bias for high-intensity regions to be net exporters and low-intensity regions to be net importers of embodied CO_2 emissions. This finding mirrors previous results [1, 2, 7, 13–18, 20, 21, 23–27]. The key difference is that our trade networks were entirely randomized. Importantly, this suggests that our findings are not a consequence of global trade relations, but an *artifact resulting from pairing unequal intensities with Leontief analysis*. Given that this is a natural research strategy for the field, the conclusion is a cautionary lesson.

Section III A discusses the primary results from our null-model MRIO table. Section III B then follows with a definition of *eco-majorization*. We show how, in the framework of Leontief analysis, it drives global flows of trade. This leads us to hypothesize the conditions under which Leontief analysis is biased towards eco-majorized results. Section III C alters the parameters of the null model to explore the consequences of relaxing these conditions. This reveals a strong relationship between both conditions—between eco-majorization and the directionality of embodied CO_2 flows.

A. Flows in the null model

We drew 1000 samples from the null model with $\zeta_{C,i}$ and ζ_X set at the baseline values $\bar{\zeta}_{C,i}$ and $\bar{\zeta}_X$. For each sample from the null model, we juxtaposed the resulting
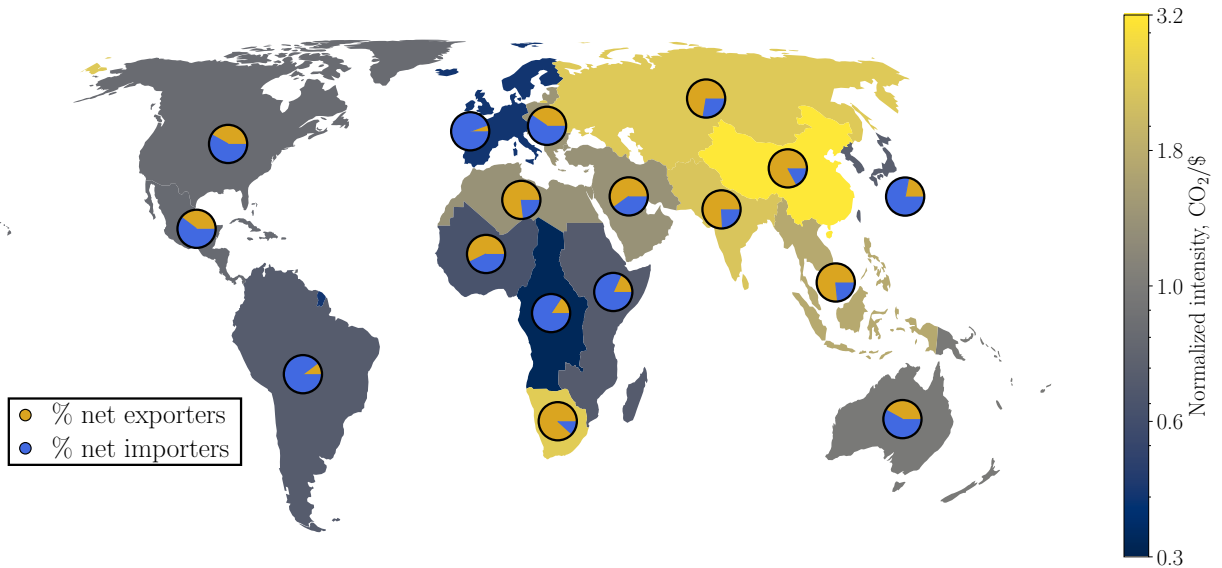
FIG. 3. Embodied CO_2 flows: Two sets of information for each of 17 megaregions. *Regional color*: Normalized intensity $\hat{f}_r^{(CO_2)}$ for each region r with bright yellow indicating higher intensities and dark blue indicating lower. *Regional pie charts*: Proportion of null models for which the given region was a net exporter (yellow) or a net importer (blue). A chart's amount of yellow corresponds to the quantity $\Xi_r^{(\alpha)}$—sample proportion of net positive exports; see text. This map uses the Equal Earth projection [54].

attribution matrix with the predetermined CO_2 intensity $\hat{\mathbf{f}}^{(CO_2)}$ and labor intensity $\hat{\mathbf{f}}^{(L)}$ to calculate the embodied flows of these impacts. For each region and impact, we calculated the proportion of samples for which the net exports $\xi_r^{(\alpha)}$ were positive, denoting the proportion $\Xi_r^{(\alpha)}$. In addition to being a function of the region r, $\Xi_r^{(\alpha)}$ is dependent on the null model parameters as well as the impact distribution $\hat{\mathbf{e}}^{(\alpha)}$, and may be termed the *null likelihood of net exports* for region r with respect to resource α. Figure 3 displays the impact intensities in color and the null export likelihood as a pie chart for each region with respect to CO_2.

Despite the null model having no preferred directionality between regions or, for that matter, even any preferred tendency between imported and domestic sources, one sees that high-intensity regions have a strong tendency to export embodied CO_2 while low-intensity regions have a strong tendency to import embodied CO_2. Moderately-intense regions do not exhibit bias.

The relationship between intensity $\hat{f}_r^{(\alpha)}$ and export likelihood $\Xi_r^{(\alpha)}$ can be expressed using a nonlinear measure of correlation, such as Kendall's τ [55]. We found that the correlation between the two quantities for carbon was $\tau^{(CO_2)} = 0.68$. While, for labor, the correlation was a remarkable $\tau^{(L)} = 0.96$. Likely, this is due to the fact that labor intensities are determined on the factor level—consequently, there is no intra-regional variation in labor intensity that confounds the relationship between

intensity and global trade.

In this way, the null models demonstrate that complete randomization of social factors in MRIO tables has little effect on the directionality of embodied flows: they are still directed from high- to low-intensity regions. The following section offers an explanation, via majorization, for how the assumptions underlying Leontief analysis itself drive the correlation between impact intensities and embodied flows.

B. Eco-majorization and Leontief bias

Majorization's key benefit is that it readily explains the internal mechanics of input-output analysis. In this way, the present use is yet another example of generalizing thermodynamic logic to new settings. Such applications have, for instance, already been powerfully applied to develop quantum resource theories, which make frequent use of majorization to study entanglement and other quantum properties as a nonfungible resources [45–49].

The following, using it, shows that Leontief analyses tends to detect flows of embodied impacts from high-intensity regions to low-intensity regions. The effect is physically analogous to particles diffusing from high-density to low-density regions. In this way, majorization connects these two settings.

Majorization is defined on probability vectors, whose

total sum is normalized to 1, but we will for simplicity write unnormalized vectors in the majorization pairs as a shorthand for the majorization of their normalized forms. We will demonstrate that if the following conditions hold for an EE-MRIO with impact α:

(MRIO-1) The regional impact intensities $\hat{\mathbf{f}}^{(\alpha)}$ are highly heterogeneous and

(MRIO-2) The regional deficit $\hat{\mathbf{x}} - \hat{\mathbf{y}}$ is small as a proportion of regional income across regions,

then with high probability Leontief analysis results in (or approximately results in) the majorization:

$$\left(\hat{\mathbf{e}}^{(\alpha)}, \hat{\mathbf{y}}\right) \succeq \left(\hat{\mathbf{a}}^{(\alpha)}, \hat{\mathbf{y}}\right) \ . \tag{8}$$

As this phenomenon links both ecological impacts and economic activity levels, we call this relation *eco-majorization*, where the prefix may refer to either. We note that both assumptions hold for the GTAP 8 dataset.

Since the regional income distribution $\hat{\mathbf{y}}$ plays a role similar to the thermodynamic Gibbs distribution, the stated relation tells us that the embodied impacts $\hat{\mathbf{a}}^{(\alpha)}$ are more similarly distributed to the regional incomes than to the local impacts $\hat{\mathbf{e}}^{(\alpha)}$. This necessitates transferring embodied impacts from high-intensity regions, where distributional imbalance is most positive, to low-intensity regions, where it is most negative.

We quantify the previous statement using net exports $\boldsymbol{\xi}^{(\alpha)}$ and impact ratios $\rho_r^{(\alpha)}$. Let $\mathcal{R}_k$ be that subset of regions containing the k regions with the highest values of $\hat{f}_r^{(\alpha)}$. Then it can be shown that, if eco-majorization holds:

$$\sum_{r \in \mathcal{R}_k} \xi_r^{(\alpha)} \geq 0 \text{ and}$$
$$\sum_{r \in \mathcal{R}_k} \frac{\hat{e}_r^{(\alpha)}}{E} \rho_r^{(\alpha)} \leq 1 \ . \tag{9}$$

Both indicators then tell us that regions in $\mathcal{R}_k$ must be net exporting or, at least, never net importing. Figure 4 presents a visual proof using Lorenz curves. Since a Lorenz curve is monotonically decreasing in slope, the curve $\beta(x)$ formed by taking only a subset of segments must always be lower in height than the original curve. From this it can be seen that when $\left(\hat{\mathbf{e}}^{(\alpha)}, \hat{\mathbf{y}}\right) \succeq \left(\hat{\mathbf{a}}^{(\alpha)}, \hat{\mathbf{y}}\right)$, we must have $\sum_{r \in \mathcal{R}_k} \hat{a}_r \leq \sum_{r \in \mathcal{R}_k} \hat{e}_r$, from which Eqs. (9) hold.

Eco-majorization, then, places rigid constraints on the directionality of trade flows. Our null model simulation decisively demonstrates it is at play in the observed relationship between intensity and exports: embodied labor
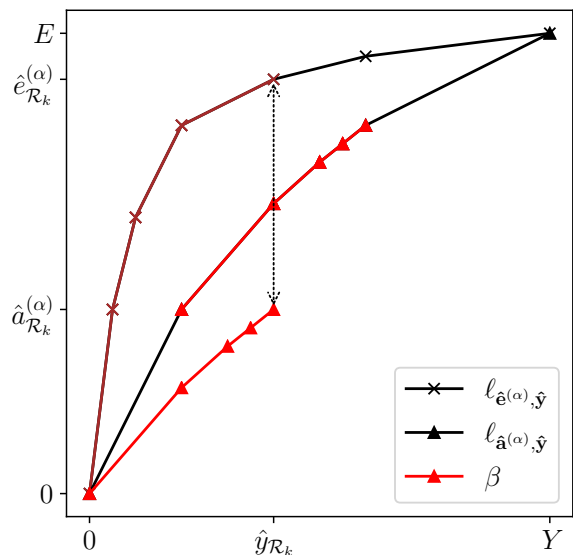

FIG. 4. Most intense regions must be net exporters: Graphical proof that, as long as eco-majorization holds, the k most intense regions $\mathcal{R}_k$ will have $\hat{\mathbf{a}}_{\mathcal{R}_k}^{(\alpha)} \leq \hat{\mathbf{e}}_{\mathcal{R}_k}^{(\alpha)}$. This rests on the fact that the partial Lorenz curve β corresponding only to the regions $\mathcal{R}_k$ must be below the Lorenz curve $\ell_{\hat{\mathbf{a}}^{(\alpha)}, \hat{\mathbf{y}}}$. And that, in turn, falls below $\ell_{\hat{\mathbf{e}}^{(\alpha)}, \hat{\mathbf{y}}}$.

flows were eco-majorized for 100% of the simulated networks and embodied CO_2 flows were eco-majorized for 72% of the simulated networks.

These results suggest that while eco-majorization is not guaranteed, it is a highly ubiquitous phenomenon among randomly generated MRIO tables. The issue, we argue, rests in the presence of the two conditions (MRIO-1) and (MRIO-2).

Due to Eqs. (6) and (S8), the BSS theorem automatically entails:

$$\left(\mathbf{e}^{(\alpha)}, \mathbf{v}\right) \succeq \left(\hat{\mathbf{a}}^{(\alpha)}, \hat{\mathbf{x}}\right) \ . \tag{10}$$

This differs from Eq. (8) in two key respects. First, the lefthand side refers to the sectoral impact distribution $\mathbf{e}^{(\alpha)}$ and the factor income distribution $\mathbf{v}$ rather than the regionalized distributions $\hat{\mathbf{y}}^{(\alpha)}$ and $\hat{\mathbf{y}}$, respectively. We call this difference *regionalization*. Second, the righthand side uses the spending distribution $\hat{\mathbf{x}}$ instead of the income distribution $\hat{\mathbf{y}}$. This is of little concern issue when the regional deficit is small, as assumed in (MRIO-2). By the nature of Lorenz curves, small changes in the underlying distributions result in correspondingly small changes in curve's shape.

The subtlety, and the only reason why 100% of simulated networks do not display majorization for all impacts, arises from regionalization: Eq. (10) shows that majorization holds for the full sectoral distributions, but does not

say anything about regional distributions. It is entirely *possible* that Eq. (10) may be true and Eq. (8) may be false. The crux of this issue is, in fact, the same as a major point of thermo-majorization theory: namely, that when the majorizing pair of distributions are coarse-grained, majorization might no longer hold. Notably, many recent results on the work cost of driving systems away from thermodynamic equilibrium exploit this phenomenon [49, 53].

We are not interested here in how to induce this phenomenon. Rather, we are interested in why it does not appear to naturally arise in either the existing trade data or the null model. Our argument is that condition (MRIO-1) significantly constrains the possible configurations that may result in a violation of Eq. (8).

The argument is as follows. For a set $\mathcal{S}$ of regions, define:

$$\hat{y}_{\mathcal{S}} := \sum_{s \in \mathcal{S}} \hat{y}_s \ ,$$

$$\hat{f}_{\mathcal{S}}^{(\alpha)} := \frac{\sum_{s \in \mathcal{S}} \hat{e}_s^{(\alpha)}/E}{\hat{y}_{\mathcal{S}}/Y} \ , \ \text{and}$$

$$\hat{f}_{\mathcal{S}}^{(\alpha)'} := \frac{\sum_{s \in \mathcal{S}} \hat{a}_s^{(\alpha)}/E}{\hat{y}_{\mathcal{S}}/Y} \ .$$

Further, let $\hat{y}_k := \hat{y}_{\mathcal{R}_k}$ for simplicity. To violate majorization there must be a set $\mathcal{S}$ of regions such that:

$$\hat{f}_{\mathcal{S}}^{(\alpha)'} \geq \left(\frac{\hat{y}_{\mathcal{S}} - \hat{y}_k}{\hat{y}_{k+1} - \hat{y}_k} \right) \hat{f}_{\mathcal{R}_k}^{(\alpha)} + \left(\frac{\hat{y}_{k+1} - \hat{y}_{\mathcal{S}}}{\hat{y}_{k+1} - \hat{y}_k} \right) \hat{f}_{\mathcal{R}_{k+1}}^{(\alpha)} \ , \ (11)$$

where k is the unique integer such that $\hat{y}_k \leq \hat{y}_{\mathcal{S}} < \hat{y}_{k+1}$. (This simply restates the definition of majorization via Lorenz curves.) We can actually suppose without loss of generality that $\hat{y}_k = \hat{y}_{\mathcal{S}}$. This can be achieved by splitting regions into smaller but structurally identical subregions. So, Eq. (11) can be expressed more simply as $\hat{f}_{\mathcal{S}}^{(\alpha)'} \geq \hat{f}_{\mathcal{R}_k}^{(\alpha)}$.

Now, we may rewrite $\hat{f}_{\mathcal{S}}^{(\alpha)'}$ as:

$$\hat{f}_{\mathcal{S}}^{(\alpha)'} = \sum_{\substack{r \in \mathcal{R} \\ i \in \mathcal{I}_0}} \frac{\hat{A}_{ri,s} y_{ri}}{\hat{y}_{\mathcal{S}}} f_{ri}^{(\alpha)} \ . \quad (12)$$

This considerably constrains the structure of matrices $\hat{\mathbf{A}}$ that yield a large value for $\hat{f}_{\mathcal{S}}^{(\alpha)'}$. Specifically, if $\hat{f}_{\mathcal{S}}^{(\alpha)'} \geq \hat{f}_{\mathcal{R}_k}^{(\alpha)}$, then $\hat{A}_{ri,s}$ either must put great weight on the most intense sectors within the regions of $\mathcal{R}_k$ or it must draw from similarly intense sectors that may, with small probability, have arisen in less intense regions. In either case, $\hat{A}_{ri,s}$ must give high weight to sectors (r, i) with intensities $f_{ri}^{(\alpha)}$ that exceed the average intensity of the highest k regions: $f_{ri} > \hat{f}_{\mathcal{R}_k}^{(\alpha)}$.

The Markov inequality states that for any positive random variable X with mean value $\hat{x}$, the probability that an instance exceeds the mean by a proportion β is constrained [56]:

$$\Pr\left(X \geq \beta \hat{x} \right) \leq \frac{1}{\beta} \ .$$

Then for each region r, the weight (under $\mathbf{v}$) that a given sectoral intensity exceeds $\hat{f}_k^{(\alpha)}$ by a proportion β is:

$$\sum_{i: f_{ri} > \beta \hat{f}_{\mathcal{R}_k}^{(\alpha)}} v_{ri} \leq \frac{q_r \hat{f}_r^{(\alpha)}}{\beta \hat{f}_{\mathcal{R}_k}^{(\alpha)}} \ .$$

Thus, due to the Markov inequality, high-intensity sectors are suppressed in weight, in a manner determined by the relative proportions of intensities between regions. When condition (MRIO-2) holds—that is, the regional intensities are highly heterogeneous—this suppression is strengthened.

To counter this suppression in Eq. (12), $\hat{A}_{ri,s}$ must place extremely high relative weight on high-intensity sectors. In this case, however, very little weight remains to distribute among other sectors. Combinatorially, then, matrices $\hat{\mathbf{A}}$ violating regional majorization occupy a relatively small niche in the space of all configurations.

To summarize, as a consequence of the BSS theorem and fundamental facts of Leontief analysis, Eq. (10) must hold for any EE-MRIO table. When assumptions (MRIO-1) and (MRIO-2) hold, implying heterogeneity of regional intensities and small regional deficits, Eq. (10) further supports eco-majorization Eq. (8) by constraining the possible configurations which are not eco-majorized.

In the analogous thermodynamic setting, the experimenter (a Maxwell's "demon") may intentionally configure matrices that violate majorization after coarse-graining. In the setting of global trade, however, such a matrix must come about as the result of a strict bias among some regions to only consume high-intensity products. This is hardly realistic: Even at a national level, imports are a function of the variegated needs of multiple consumers and corporations. And, they necessarily draw their consumption from high-intensity and low-intensity industries. Regions, in short, do not operate as Maxwellian demons—at least, not in regards to their bulk imports.

Furthermore, as the null model is symmetrically generated without knowledge of local intensities, the null model is not be likely to draw models from the small niche required significantly violate majorization. Indeed, it is worth noting that our null model effectively acts as a Monte-Carlo model, calculating the total probability mass of the configuration space where majorization is violated.
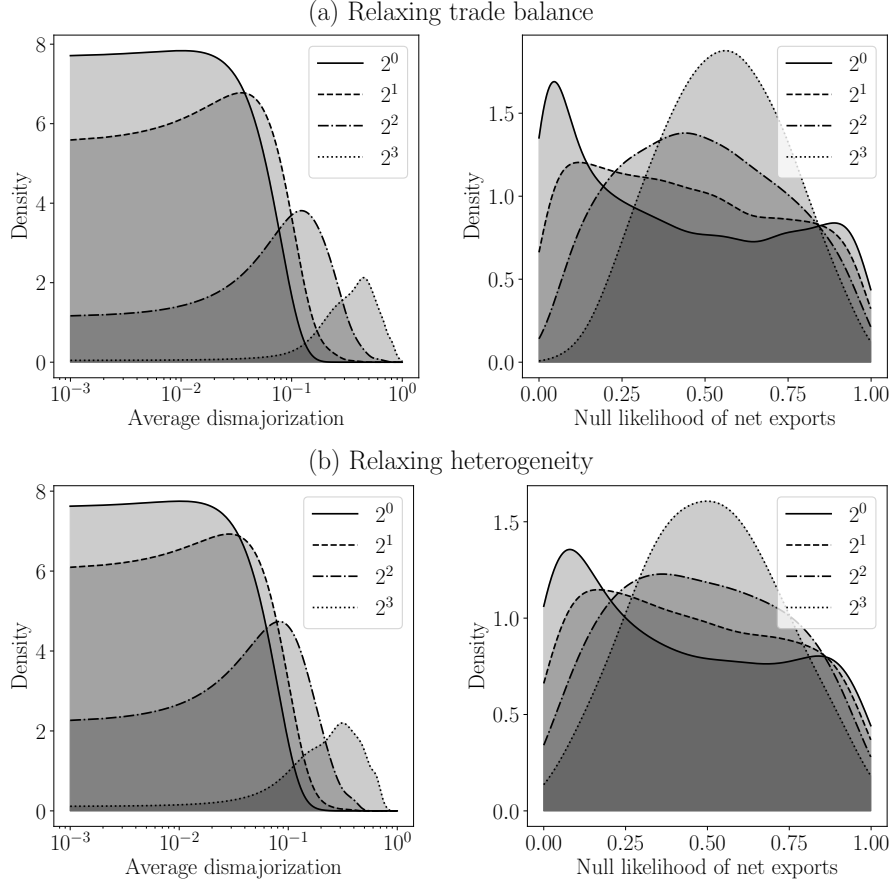
FIG. 5. Emergence of eco-majorization: The results of varying the conditions that, when paired with Leontief analysis, result in eco-majorization. *(a)* Relaxing trade balance: Four suites of ensembles where the trade balance parameter was taken as $\zeta_X = \sigma^{-1}\zeta_X$, $\sigma = 2^0, 2^1, 2^2, 2^3$. As σ grows, so does the ensemble's overall trade deficit. A Gaussian kernel density was computed for the dismajorization and the null likelihood of net export over the null model samples. The left plot demonstrates that trade deficit's increase has the effect of increasing the average dismajorization. The right plot demonstrates that this also has the impact of shifting the net export density from being bimodal to unimodal. *(b)* Relaxing heterogeneity: Four suites of ensembles where the impact heterogeneity parameter was taken as $\zeta_U = \sigma\zeta_U$, $\sigma = 2^0, 2^1, 2^2, 2^3$. As σ grows, heterogeneity decreases. This has similar effects on the dismajorization density plot and the net export density plot.

C.   Relaxing assumptions

To verify that conditions (MRIO-1) and (MRIO-2) are indeed responsible for the appearance of majorization and, consequently, the coupling between intensities and embodied flows, we made two modifications to the null model. First, we introduced null-impact intensities. Second, we varied parameters of both the MRIO null model and the impact intensity null model to determine their effects. We performed these in two separate trials.

For the first, we generated 1000 unobtainium intensity functions with parameter $\zeta_U = \bar{\zeta}_U$. For each scaling factor $\sigma = 1, 2, 4, 8$, we generated 250 MRIO tables from the null model with $\boldsymbol{\zeta_C} = \bar{\boldsymbol{\zeta}}_C$ and $\zeta_X = \sigma^{-1}\bar{\zeta}_X$. This results in 4 ensembles of $250,000$ EE-MRIO tables each, with increasing trade imbalances from one ensemble to the next.

For the second, we flipped the structure of this approach, generating 1000 MRIO tables from the null model with $\boldsymbol{\zeta_C} = \bar{\boldsymbol{\zeta}}_C$ and $\zeta_X = \bar{\zeta}_X$. Then, for each scaling factor $\sigma = 1, 2, 4, 8$, we generated 250 unobtainium intensities with parameter $\zeta_U = \sigma\bar{\zeta}_U$. This results in the same number of ensembles, but with decreasing heterogeneity of intensities.

To quantify the effect of the changes in parameter on majorization, we used dismajorization $\mathrm{DM}\left[(\hat{\mathbf{e}}^{(\mathrm{U})}, \hat{\mathbf{y}}); (\hat{\mathbf{a}}^{(\mathrm{U})}, \hat{\mathbf{y}})\right]$, as defined in Section II C. For the first suite of ensembles, for every sampled MRIO table we calculated the average dismajorization over all unobtainum distributions. Then, a density plot of average dismajorizations over all samples with a given scaling factor σ was computed. The resulting density functions are shown in Fig. 5. Similarly, for the second suite, for every sampled unobtainium distribution we calculated the

average dismajorization over all MRIO tables. Density plots were similarly taken for each scaling factor σ. The resulting density functions are also shown in Fig. 5. We find in each case that the likely dismajorization increases dramatically as the assumptions (MRIO-1) and (MRIO-2) are relaxed.

For both suites, we also sought to examine the impact of the scaling factors on trade-flow directionality. To this end, we calculated the null likelihoods of net exports Ξ_r for each region and each unobtainium distribution $\hat{\mathbf{e}}^{(U)}$. We made a density plot of observed values of Ξ_r for each value of $\sigma = 1, 2, 4, 8$. At the baseline parameter values ($\sigma = 1$), this density plot is bimodal, with one mode close to zero (countries that tend to be net importers) and one mode close to one (those that tend to be net exporters). However, as the baseline values are altered to relax assumptions, the density of Ξ_r becomes unimodal—the sharp distinction between exporters and importers vanishes. This is true as either assumption is relaxed.

These results complement those of the previous section. In Section III B we showed that that the assumptions (MRIO-1) and (MRIO-2) are together sufficient for majorization to be predominant; Fig. 5 shows that they are each necessary. Additionally, relaxing either assumption (and the consequent irrelevancy of majorization) diminishes an initially strong dichotomy between exporting and importing nations, as the density of Ξ_r goes from bimodal to unimodal.

IV.   DISCUSSION & CONCLUDING REMARKS

The two assumptions of Leontief analysis, (L-1) and (L-2), are critically important for understanding (i) the emergence of majorization in this setting and (ii) how exploring the validity of Leontiefian assumptions has great merit in assessing its results' usefulness. The "foothold" that majorization makes in our analysis begins with Eqs. (6) and (S8):

$$\mathbf{v}\hat{\mathbf{A}} = \hat{\mathbf{x}} \text{ and}$$
$$\mathbf{e}^{(\alpha)}\hat{\mathbf{A}} = \hat{\mathbf{a}}^{(\alpha)} \ .$$

These equations relate factor incomes to the regional spending and production impacts to attributed impacts. Since both use the same attribution matrix $\hat{\mathbf{A}}$, the initial majorization relation Eq. (10) holds. Our mathematical analysis rests on this fact.

In information theory, stochastic matrices act as lossy channels that transmit information in a degraded condition. This leads distinct channel inputs to become more similar. While we sorted out the subtleties here, it is primarily for this reason that embodied emissions become more similar to global income: they are both channeled through the same lines of flow, determined by the single matrix $\hat{\mathbf{A}}$.

However, employing the same attribution matrix—whose primary determinant is *monetary* flows—to also drive embodied impact flows is a possibility only allowed by (L-1) and (L-2). The homogeneity of products and prices allows us to assume that monetary flows are entirely sufficient to reconstruct the commodity chains in which embodied flows are materialized. Without these assumptions, one would have a unique attribution matrix $\hat{\mathbf{A}}^{(\alpha)}$ for each impact α, distinct from the monetary attribution matrix. Majorization would no longer necessarily hold. And so, it would no longer drive the relationship between local intensities and embodied flows. In this way, our results suggest that the outcomes of Leontief analysis are highly dependent on the assumptions made. Rather than a neutral tool of analysis, Leontiefian methods embody significant ideological consequences.

Consider in this light the carbon leakage hypothesis. Essentially, firms from high-income countries foist the direct carbon costs of their production (which feeds local consumption) onto lower-income countries. This maintains consumption patterns while lowering compliance costs by superficially adhering to climate treaties to which they are signatories [1, 2].

When this extends beyond carbon to other environmental impacts, the flow of embodied impacts from low- to high-income countries is *ecologically unequal exchange*—a major topic in modern geography and ecological economics [3–6]. One can even consider impacts such as labor-time. This leads to the more traditional hypothesis of unequal exchange [57] of exploited labor from low- to high-income countries. Each of these hypotheses rests on fundamental assumptions about the social and economic power relations between nations and regions.

Multiregional input-output tables and Leontief analysis have been put to use evaluating these hypotheses previously, frequently in tandem with quantities such as the net exports $\boldsymbol{\xi}^{(\alpha)}$ and consumption-to-production ratio $\boldsymbol{\rho}^{(\alpha)}$ which we have analyzed here [7, 15, 17, 19–21, 23–27]. Our results directly bear on these previous studies. We showed that these quantities are, in fact, strongly driven by the assumptions of Leontief analysis and are largely independent of the relational data within the MRIO tables used. This calls into question the validity of Leontief analysis as a tool for empirically verifying hypotheses of unequal exchange, contributing a new perspective to previous critiques of this application [24].

Employing MRIO tables and Leontief analysis for empirical purposes must be done with caution. To this end,

we recommend an approach based on that taken here. Specifically, for this we make two contributions. First, use modern tools from information theory and statistical physics to better understand the consequences of methods like Leontief analysis, embedded as they are with numerous stochastic matrices and distributional relationships. Second, frequently consult with null models. This will aid in disentangling data structures, mathematical artifacts, and hypotheses, as otherwise these can be quite difficult to tease apart when using sophisticated modeling assumptions. This recommendation, of course, extends beyond MRIO tables and Leontief analysis. However, applying this approach to other studies of carbon accounting, environmental impacts, and ecologically unequal exchange will remain for future work.

ACKNOWLEDGMENTS

REPRODUCIBILITY STATEMENT

To contribute to the methods' reproducibility, we provide the scripts and Jupyter Notebooks used to perform our analysis in a Github repository [58]. The code makes use of the package `stoclust`, a tool for ensemble-based statistical analysis [59]. The source data must be acquired from GTAP 8, the most recent freely accessible version of GTAP [51, 60].

[1] Glen P. Peters, Jan C. Minx, Christopher L. Weber, and Ottmar Edenhofer. Growth in emission transfers via international trade from 1990 to 2008. *PNAS*, 108(21):8903–8908, May 2011. Publisher: National Academy of Sciences Section: Biological Sciences. 1, 6, 11

[2] Steven J. Davis, Glen P. Peters, and Ken Caldeira. The supply chain of CO2 emissions. *PNAS*, 108(45):18554–18559, November 2011. Publisher: National Academy of Sciences Section: Biological Sciences. 1, 6, 11

[3] Alf Hornborg. The Unequal Exchange of Time and Space: Toward a Non-Normative Ecological Theory of Exploitation. *Journal of Ecological Anthropology*, 7(1):4–10, January 2003. 1, 11

[4] James Rice. Ecological Unequal Exchange: Consumption, Equity, and Unsustainable Structural Relationships within the Global Economy. *International Journal of Comparative Sociology*, 48(1):43–72, February 2007. Publisher: SAGE Publications Ltd.

[5] David A. Smith. Trade, unequal exchange, global commodity chains. In *Routledge Handbook of World-Systems Analysis*. Routledge, May 2012.

[6] Andrew K. Jorgenson and James Rice. The sociology of ecologically unequal exchange in comparative perspective. In *Routledge Handbook of World-Systems Analysis*. Routledge, May 2012. 11

[7] Luke Bergmann. Bound by Chains of Carbon: Ecological–Economic Geographies of Globalization. *Annals of the Association of American Geographers*, 103(6):1348–1370, November 2013. 1, 4, 6, 11

[8] Wassily Leontief. The economy as a circular flow. *Structural Change and Economic Dynamics*, 2(1):181–212, June 1991. 1, 3, 2

[9] Wassily Leontief. *Essays in Economics: Theories, Theorizing, Facts, and Policies*. Transaction Publishers, 1966. 3, 2

[10] Thomas Wiedmann. Editorial: Carbon Footprint and Input–Output Analysis – an Introduction. *Economic Systems Research*, 21(3):175–186, September 2009. Publisher: Routledge _eprint: https://doi.org/10.1080/09535310903541256. 4

[11] Justin Kitzes. An Introduction to Environmentally-Extended Input-Output Analysis. *Resources*, 2(4):489–503, December 2013. Number: 4 Publisher: Multidisciplinary Digital Publishing Institute. 1, 2

[12] Anke Schaffartzik, Magdalena Sachs, Dominik Wiedenhofer, and Nina Eisenmenger. Market Interaction and Efficient Cooperation. Technical Report 154, Institute of Social Ecology, IFF, Vienna, 2014. 1, 2, 3

[13] Fridolin Krausmann, Karl-Heinz Erb, Simone Gingrich, Christian Lauk, and Helmut Haberl. Global patterns of socioeconomic biomass flows in the year 2000: A comprehensive assessment of supply, consumption and constraints. *Ecological Economics*, 65(3):471–487, April 2008. 1, 6

[14] Glen P. Peters. From production-based to consumption-based national emission inventories. *Ecological Economics*, 65(1):13–23, March 2008.

[15] Karl-Heinz Erb, Fridolin Krausmann, Wolfgang Lucht, and Helmut Haberl. Embodied HANPP: Mapping the spatial disconnect between global biomass production and consumption. *Ecological Economics*, 69(2):328–334, December 2009. 4, 11

[16] Daniel D. Moran, Mathis C. Wackernagel, Justin A. Kitzes, Benjamin W. Heumann, Doantam Phan, and Steven H. Goldfinger. Trading spaces: Calculating embodied Ecological Footprints in international trade using a Product Land Use Matrix (PLUM). *Ecological Economics*, 68(7):1938–1951, May 2009.

[17] Steven J. Davis and Ken Caldeira. Consumption-based accounting of CO2 emissions. *PNAS*, 107(12):5687–5692, March 2010. Publisher: National Academy of Sciences Section: Biological Sciences. 4, 11

[18] Thomas Wiedmann, Richard Wood, Jan C. Minx, Manfred Lenzen, Dabo Guan, and Rocky Harris. A Carbon Footprint Time Series of the Uk – Results from a Multi-Region Input–Output Model. *Economic Systems Research*, 22(1):19–42, March 2010. Publisher: Routledge _eprint: https://doi.org/10.1080/09535311003612591. 6

[19] Daniel D. Moran, Manfred Lenzen, Keiichiro Kanemoto, and Arne Geschke. Does ecologically unequal exchange occur? *Ecological Economics*, 89:177–186, May 2013. 4, 11

[20] Yang Yu, Kuishuang Feng, and Klaus Hubacek. Teleconnecting local consumption to global land use. *Global Environmental Change*, 23(5):1178–1186, October 2013. 4, 6

[21] Ali Alsamawi, Joy Murray, and Manfred Lenzen. The Employment Footprints of Nations. *Journal of Industrial Ecology*, 18(1):59–70, 2014. _eprint: https://onlinelibrary.wiley.com/doi/pdf/10.1111/jiec.12104. 4, 6, 11

[22] Christina Prell, Kuishuang Feng, Laixiang Sun, Martha Geores, and Klaus Hubacek. The Economic Gains and Environmental Losses of US Consumption: A World-Systems and Input-Output Approach. *Social Forces*, 93(1):405–428, September 2014. 4

[23] Moana S. Simas, Laura Golsteijn, Mark A. J. Huijbregts, Richard Wood, and Edgar G. Hertwich. The "Bad Labor" Footprint: Quantifying the Social Impacts of Globalization. *Sustainability*, 6(11):7514–7540, November 2014. Number: 11 Publisher: Multidisciplinary Digital Publishing Institute. 4, 6, 11

[24] Christian Dorninger and Alf Hornborg. Can EEMRIO analyses establish the occurrence of ecologically unequal exchange? *Ecological Economics*, 119:414–418, November 2015. 11

[25] Hongguang Liu, Weidong Liu, Xiaomei Fan, and Zhigao Liu. Carbon emissions embodied in value added chains in China. *Journal of Cleaner Production*, 103:362–370, September 2015.

[26] Luke Bergmann and Mollie Holmberg. Land in Motion. *Annals of the American Association of Geographers*, 106(4):932–956, July 2016. 4

[27] Azusa Oita, Arunima Malik, Keiichiro Kanemoto, Arne Geschke, Shota Nishijima, and Manfred Lenzen. Substantial nitrogen pollution embedded in international trade. *Nature Geoscience*, 9(2):111–115, February 2016. Number: 2 Publisher: Nature Publishing Group. 4, 6, 11

[28] Jan Oosterhaven. Basic, Demand-Driven IO Quantity Models. In Jan Oosterhaven, editor, *Rethinking Input-Output Analysis: A Spatial Perspective*, SpringerBriefs in Regional Science, pages 5–18. Springer International Publishing, Cham, 2019. 1, 2

[29] *Environmental Accounts of the Netherlands, 2012*. Statistics Netherlands, The Hague, 2012. 1

[30] *Industrial Development Report 2016: The Role of Technology and Innovation in Inclusive and Sustainable Industrial Development*. United Nations Industrial Development Organization, Vienna, 2015.

[31] *Renewable Energy Jobs: Future Growth in Australia*. Climate Council of Australia Ltd., 2016.

[32] World Bank Group. *World Development Report 2020: Trading for Development in the Age of Global Value Chains*. International Bank for Reconstruction and Development / The World Bank, Washington, D. C., 2020. 1

[33] Anke Schaffartzik, Dominik Wiedenhofer, and Nina Eisenmenger. Raw Material Equivalents: The Challenges of Accounting for Sustainability in a Globalized World. *Sustainability*, 7(5):5345–5370, May 2015. Number: 5 Publisher: Multidisciplinary Digital Publishing Institute. 1

[34] Hal Whitehead. Investigating structure and temporal scale in social organizations using identified individuals. *Behavioral Ecology*, 6(2):199–208, December 1995. 1, 4

[35] M. Ángeles Serrano, Marián Boguñá, and Romualdo Pastor-Satorras. Correlations in weighted networks. *Phys. Rev. E*, 74(5):055101, November 2006. Publisher: American Physical Society. 4

[36] Gerrit Ansmann and Klaus Lehnertz. Constrained randomization of weighted networks. *Phys. Rev. E*, 84(2):026103, August 2011. Publisher: American Physical Society. 4

[37] Brenton J. Prettejohn, Matthew J. Berryman, and Mark D. McDonnell. Methods for Generating Complex Networks with Selected Structural Properties for Simulations: A Review and Tutorial for Neuroscientists. *Front. Comput. Neurosci.*, 5, 2011. Publisher: Frontiers. 4

[38] Robert W. Rankin, Janet Mann, Lisa Singh, Eric M. Patterson, Ewa Krzyszczyk, and Lars Bejder. The role of weighted and topological network information to understand animal social networks: a null model approach. *Animal Behaviour*, 113:215–228, March 2016. 4

[39] Damien R. Farine. A guide to null models for animal social network analysis. *Methods in Ecology and Evolution*, 8(10):1309–1320, 2017. _eprint: https://besjournals.onlinelibrary.wiley.com/doi/pdf/10.1111/2041-210X.12772. 1, 4

[40] Albert W. Marshall, Ingram Olkin, and Barry C. Arnold. *Inequalities: Theory of Majorization and Its Applications*. Springer Series in Statistics. Springer-Verlag, New York, 2 edition, 2011. 2, 5

[41] M. O. Lorenz. Methods of Measuring the Concentration of Wealth. *Publications of the American Statistical Association*, 9(70):209–219, 1905. Publisher: [American Statistical Association, Taylor & Francis, Ltd.]. 2, 5

[42] Arthur F. Veinott. Least d-Majorized Network Flows with Inventory and Statistical Applications. *Management Science*, 17(9):547–567, May 1971. Publisher: INFORMS.

2, 5

[43] David Blackwell. Comparison of Experiments. *Proceedings of the Second Berkeley Symposium on Mathematical Statistics and Probability*, pages 93–102, January 1951. Publisher: University of California Press. 2, 5

[44] David Blackwell. Equivalent Comparisons of Experiments. *The Annals of Mathematical Statistics*, 24(2):265–272, 1953. Publisher: Institute of Mathematical Statistics. 2, 5

[45] D. Janzing, P. Wocjan, R. Zeier, R. Geiss, and Th. Beth. Thermodynamic Cost of Reliability and Low Temperatures: Tightening Landauer's Principle and the Second Law. *International Journal of Theoretical Physics*, 39(12):2717–2753, December 2000. 2, 5, 7

[46] R. Horodecki, P. Horodecki, M. Horodecki, and K. Horodecki. Quantum entanglement. *Rev. Mod. Phys.*, 81:865, 2009.

[47] Fernando G. S. L. Brandão, Michał Horodecki, Jonathan Oppenheim, Joseph M. Renes, and Robert W. Spekkens. Resource Theory of Quantum States Out of Thermal Equilibrium. *Phys. Rev. Lett.*, 111(25):250404, December 2013. Publisher: American Physical Society. 6

[48] Michał Horodecki and Jonathan Oppenheim. Fundamental limitations for quantum and nanoscale thermodynamics. *Nature Communications*, 4(1):2059, June 2013. Number: 1 Publisher: Nature Publishing Group. 6

[49] Fernando Brandão, Michał Horodecki, Nelly Ng, Jonathan Oppenheim, and Stephanie Wehner. The second laws of quantum thermodynamics. *PNAS*, 112(11):3275–3279, March 2015. Publisher: National Academy of Sciences Section: Physical Sciences. 2, 6, 7, 9

[50] Sadamori Kojaku and Naoki Masuda. Core-periphery structure requires something else in the network. *New J. Phys.*, 20(4):043012, April 2018. Publisher: IOP Publishing. 4

[51] Badri Narayanan G., Angel Aguiar, and Robert McDougall. *Global Trade, Assistance, and Production: The GTAP 8 Data Base*. Center for Global Trade Analysis, Purdue University, 2012. 4, 12

[52] Terrie L Walmsley and S Amer Ahmed. A Global Bilateral Migration Data Base: Skilled Labor, Wages and Remittances. page 32, 2007. 4

[53] J. M. Renes. Relative submajorization and its use in quantum resource theories. *J. Math. Phys.*, 57:122202, 2016. 5, 6, 9

[54] Bojan Šavrič, Tom Patterson, and Bernhard Jenny. The Equal Earth map projection. *International Journal of Geographical Information Science*, 33(3):454–465, March 2019. Publisher: Taylor & Francis _eprint: https://doi.org/10.1080/13658816.2018.1504949. 7

[55] M. G. Kendall. A new measure of rank correlation. *Biometrika*, 30(1-2):81–93, 1938. 7

[56] T. M. Cover and J. A. Thomas. *Elements of Information Theory*. Wiley-Interscience, New York, second edition, 2006. 9, 6

[57] Arghiri Emmanuel. *Unequal Exchange: A Study of the Imperialism of Trade*. Monthly Review Press, 1972. 11

[58] Samuel P. Loomis. Nonequilibrium thermodynamics and carbon accounting methods. `https://github.com/samlikesphysics/netacam_code`, 2020. 12

[59] Samuel P. Loomis. stoclust python package. `https://samlikesphysics.github.io/stoclust/`, 2020. 12

[60] Global trade aggregation project. `https://www.gtap.agecon.purdue.edu/`, 2021. 12

Supplementary Materials

Nonequilibrium Thermodynamics in Measuring Carbon Footprints:
Disentangling Structure and Artifact in
Input-Output Accounting

Samuel P. Loomis, Mark Cooper, and James P. Crutchfield

In these appendices we discuss further background on input-output analysis and the construction of our null model.

Appendix A: Input-output analysis, in further detail

1. Basic input-output analysis

An *economy* $(\mathcal{I}, \mathcal{V}, \mathcal{D})$ is composed of finite sets of industrial sectors $\mathcal{I}$, value-added sectors $\mathcal{V}$, and final demand sectors $\mathcal{D}$. Value-added sectors usually include factors of production, such as labor, capital, land, and natural resources. Final demand sectors indicate the various forms of consumption: traditionally, private consumption, government spending, and business investment.

An economy's operation is cast as various kinds of *flow* between the sectors. To capture these for an economy, an input-output table is defined as the triple $(\mathbf{Z}, \mathbf{V}, \mathbf{D})$ of matrices with interindustry flows Z_{ij} $(i, j \in \mathcal{I})$; value-added flows V_{ui} $(i \in \mathcal{I}, u \in \mathcal{V})$; and final-demand flows D_{ia}, $(i \in \mathcal{I}, a \in \mathcal{D})$. Interindustry flows describe transactions between industrial firms; value-added flows describe factor returns such as wages, profits, and rent; final-demand flows describe the direct spending by individuals, governments, and businesses on consumable commodities, services, and fixed capital.

Each matrix component describes the flow of money from the column sector to the row sector over a given time period (typically a year). For instance, Z_{ij} describes the total flow of money from sector j to sector i. Each industrial sector is assumed to be balanced, so that the total outlays equal the total output:

$$\underbrace{\sum_{u \in \mathcal{V}} V_{ui} + \sum_{j \in \mathcal{I}} Z_{ji}}_{\text{Outlays}} = \underbrace{\sum_{j \in \mathcal{I}} Z_{ij} + \sum_{a \in \mathcal{D}} D_{ia}}_{\text{Outputs}} \tag{S1}$$

We define, respectively, the total output z_i of industry i, total income total demand v_i of industry i, and total value-added d_i by industry i as follows:

$$z_i := \sum_{j \in \mathcal{I}} Z_{ij} + \sum_{a \in \mathcal{D}} D_{ia}, v_i := \sum_{u \in \mathcal{V}} V_{ui}, \text{ and } d_i := \sum_{a \in \mathcal{D}} D_{ia} . \tag{S2}$$

We additionally define the total income as $Y := \sum_i v_i$, which is necessarily equal to the total spending $\sum_i d_i$ by Eq. (1).

A primary use of input-output analysis is to attribute the impacts of various activities to each of the final demand sectors. This provides a useful way to conceptualize the complex economy's interconnected causal relationships. To do this, we first define the technical coefficients C_{ij} as $C_{ij} := Z_{ij}/z_j$. These specify the outlays on activity i required to produce a single monetary unit of output in sector j. Equation (1)'s balance condition can then be written in matrix form as $\mathbf{z} = \mathbf{C}\mathbf{z} + \mathbf{d}$, a linear algebra problem whose solution (for $\mathbf{z}$) is:

$$\mathbf{z} = (\mathbf{I} - \mathbf{C})^{-1} \mathbf{d} , \tag{S3}$$

where $\mathbf{I}$ is the identity matrix and one uses the matrix inverse. Written more explicitly we have:

$$z_i = \sum_{a \in \mathcal{D}} \left[(\mathbf{I} - \mathbf{C})^{-1} \mathbf{D} \right]_{ia} . \tag{S4}$$

This expresses the total output as a column-sum of the matrix $(\mathbf{I} - \mathbf{C})^{-1} \mathbf{D}$. The sum allows us to break sector i's total output into parts, each attributed to a particular final demand $a \in \mathcal{D}$. The attribution matrix $\mathbf{A}$:

$$A_{ia} := \frac{\left[(\mathbf{I} - \mathbf{C})^{-1} \mathbf{D} \right]_{ia}}{z_i} , \tag{S5}$$

describes, for each dollar of output in sector i, how much of that dollar is attributed to final demand a. Determining these attributions is called *Leontief analysis* after its originator [8, 9].[2]

It will be important, later, to note that $\sum_a A_{ia} = 1$. When this property holds for a matrix, in addition to the condition of nonnegative components, we say the matrix is *stochastic*. It has considerable importance for majorization.

The utility of Leontief analysis rests on two main assumptions [12]:

(L-1) Sectors produce homogeneous products: Due to this, we do not reweight the technical coefficients to reflect differences between the purchasing sectors—they purchase the same item.

(L-2) Sectoral products are homogeneously priced: Every buyer pays the same unit price. This again allows using the technical coefficients without modification to reflect differences in the inputs required per dollar for different purchasers.

The text discusses these further.

2. Multiregional models

Multiregional input-output (MRIO) tables deepen the structure of input-output tables by dividing sectors into regions [9]. Specifically, we suppose there is a finite set $\mathcal{R}$ of regions and each set of sectors is organized as $\mathcal{I} = \mathcal{R} \times \mathcal{I}_0$, $\mathcal{V} = \mathcal{R} \times \mathcal{V}_0$, and $\mathcal{D} = \mathcal{R} \times \mathcal{D}_0$, where $\mathcal{I}_0$, $\mathcal{V}_0$, and $\mathcal{D}_0$ are the regional-level industrial, value-added, and final-demand sectors, respectively. An economy with this structure is said to be a *multiregional economy*.

The matrices and vectors described above can be adapted to this geographic picture by replacing each individual index $i \in \mathcal{I}$ (or others) with the pair (r, i), $r \in \mathcal{R}$ and $i \in \mathcal{I}_0$. This corresponds to re-envisioning the matrices and vectors as block-matrices and block-vectors, with rows and columns organized by regional blocks. See Fig. 1.

Simplifications are often imposed on MRIO tables. For instance, the inter-industry flows $Z_{ri,sj}$ may involve considerable inter-regional interaction, but it is typically supposed that $V_{ru,si} = 0$ and $D_{ri,sa} = 0$ whenever $r \neq s$. In other words, regional factors are paid directly by a same-region industrial sector and regional consumption purchases directly from a same-region sector. (The direct consumption of imports is addressed by introducing intra-regional importing sectors to mediate the inter-regional interaction, usually doubling the size of $\mathcal{I}_0$.) This makes $\mathbf{V}$ and $\mathbf{D}$ block-diagonal.

Three concepts are important when identifying majorization. First, while global income and global spending equal one another, it is not necessarily the case that regional income and regional spending are equal. In fact, this difference is directly related to the trade deficit, by Eq. (1). Denoting the regional income $\hat{y}_r := \sum_i v_{ri}$, the regional spending $\hat{x}_r := \sum_i d_{ri}$, and the inter-regional trade $\hat{Z}_{rs} := \sum_{ij} Z_{ri,sj}$, we have:

$$\underbrace{\hat{y}_r - \hat{x}_r}_{\text{Income} - \text{Spending}} = \underbrace{\sum_{s \in \mathcal{R}} \left(\hat{Z}_{rs} - \hat{Z}_{sr} \right)}_{\text{Exports} - \text{Imports}} .$$

We will refer to $\hat{\mathbf{y}} - \hat{\mathbf{x}}$ as simply the *regional deficit vector*. Its properties will be important in our study of majorization in Leontief analysis.

---

[2] The analysis may be reversed to attribute outputs to factors $\mathcal{Y}$ rather than to final demands $\mathcal{D}$. While not explicitly considered here, the results derived for demand-based accounting apply symmetrically to factor-based accounting.

Second, when using MRIO tables to attribute economic activities to their corresponding demands, considerably more focus is given to the region of demand than the actual sector. Presently, this is our entire concern. We therefore define the regional attribution matrix $\hat{\mathbf{A}}$ as:

$$\hat{A}_{ri,s} := \sum_{a \in \mathcal{D}_0} A_{ri,sa} \ ,$$

where $\mathbf{A}$ is the block-matrix form of the attribution matrix defined in Eq. (4). In $\hat{\mathbf{A}}$, the rows are block-structured by regions, while the each column directly corresponds to a unique region. $\hat{\mathbf{A}}$ retains the stochastic property.

Third, a profoundly important identity emerges when applying the regional attributions matrix to the value-added vector from Eq. (S2): we arrive at the regional spending vector $\hat{x}_r$:

$$\mathbf{v}\hat{\mathbf{A}} = \hat{\mathbf{x}} \ . \tag{S6}$$

This follows from the relation:

$$\frac{v_{ri}}{z_{ri}} = 1 - \sum_{\substack{s \in \mathcal{R} \\ j \in \mathcal{I}_0}} C_{sj,ri} \ ,$$

that, in turn, is a consequence of Eq. (1). What Eq. (S6) tells us is that the total value of the income for which each region's consumption is responsible is just that region's spending. And, this is the only consistent attribution if global income is to equal global spending. Leontiefian assumptions (L-1) and (L-2) suppose that environmental impacts may be attributed along the same lines as monetary flows. The fact that $\hat{A}_{ri,s}$ accurately attributes income to spending is a reflection of these assumptions and plays a central role in the appearance of majorization.

3. Environmentally extended tables

As mentioned already, we wish to explore the use of MRIO tables to attribute the impacts of economic activities to the demand sectors that stimulate them. Impacts themselves are often accounted for by environmentally extending the input-output table. A MRIO table with environmental extension is an *environmentally-extended* MRIO (EE-MRIO) table.

In the multiregional setting, an environmental extension is a family of block vectors $\{\mathbf{e}^{(\alpha)}\}$, indexed by impact α, with the form $e_{ri}^{(\alpha)}$, $r \in \mathcal{R}$ and $i \in \mathcal{I}_0$. The quantity $e_{ri}^{(\alpha)}$ gives the total impact of the activity in sector i and region r during the same time period as the other input-output matrices. For instance, if α corresponds to greenhouse gas emissions, then $e_{ri}^{(\alpha)}$ is the quantity of greenhouse gases emitted measured in carbon dioxide equivalents. The regional impacts are then given by $\hat{e}_r^{(\alpha)} = \sum_i e_{ri}^{(\alpha)}$ and the total impacts are denoted $E^{(\alpha)} = \sum_r \hat{e}_r^{(\alpha)}$.

Given impact α, we define the α-*intensity* $f_{ri}^{(\alpha)}$ of sector (r, i) as the ratio of environmental impact to economic impact. While there are many different definitions, for our needs we define it as:

$$f_{ri}^{(\alpha)} := \frac{e_{ri}^{(\alpha)}/v_{ri}}{E^{(\alpha)}/Y} \ .$$

That is, we take the ratio of the impact $e_{ri}^{(\alpha)}$ to the *value-added* v_{ri} by sector (r, i). This directly relates the emission at a given stage of production to the value added to the region by that production. (Not counted in this is the economic input from other industries, as this value has already been counted as value-added in another industry.) To remove dependence on the units used, we normalize the ratio by comparing it to the total ratio between emissions and income.

We can similarly define the *regional intensity* by

$$\hat{f}_r^{(\alpha)} := \frac{\hat{e}_r^{(\alpha)}/\hat{y}_r}{E^{(\alpha)}/Y} \tag{S7}$$

$$= \sum_{i \in \mathcal{I}_0} \frac{v_{ri}}{\hat{y}_r} f_{ri}^{(\alpha)} \ .$$

As Eq. (S7) indicates, this can be conceptualized either as a ratio of totals or the regional average of sectoral intensities. Impacts happen at the point of production, but this activity meets a demand somewhere potentially geographically distant. Impacts may be thought of as becoming *embodied* in their product, which travels from production to demand [10]. EE-MRIO tables have been frequently used to compute the flow of embodied impacts from production to final demand. While impact at the point of production is described the impacts vector $\hat{\mathbf{e}}^{(\alpha)}$, the embodied impacts attributed to each region r are given by the attribution vector:

$$\hat{\mathbf{a}}^{(\alpha)} := \mathbf{e}^{(\alpha)}\hat{\mathbf{A}} \ . \tag{S8}$$

In theory, the quantity $\hat{a}_r^{(\alpha)}$ describes the total impact, originating anywhere in the global economy, required to meet the demands of region r. We again emphasize that this depends on the assumptions (L-1) and (L-2). For now, it is sufficient to appreciate that these are the standard calculations employed in Leontief analysis of EE-MRIO tables.

Embodied flows resulting from Leontief analysis are frequently quantified by one or both of the following proxy measures [7, 15, 17, 19–21, 23–27]:

1. The net export $\boldsymbol{\xi}^{(\alpha)} = (\xi_r^{(\alpha)})$ of attributed impact, as a share of total global impact:

$$\xi_r^{(\alpha)} = \frac{\hat{e}_r^{(\alpha)} - \hat{a}_r^{(\alpha)}}{\sum_r \hat{e}_r^{(\alpha)}} \ .$$

2. Or, the ratio $\boldsymbol{\rho}^{(\alpha)} = (\rho_r^{(\alpha)})$ of attributed impact to direct impact:

$$\rho_r^{(\alpha)} = \frac{\hat{a}_r^{(\alpha)}}{\hat{e}_r^{(\alpha)}} \ .$$

Naturally, these are closely related, as they ultimately express the relationship between the relative sizes of produced impacts and consumed impacts.

Appendix B: Null model construction

The structure of the null model is primarily founded on a distinction among the technical coefficients, between those that are truly "technical" (in that they depend directly on production techniques) and those that are "social" (in that they may depend on exogenous social parameters, such as acceptable wage levels, trade agreements, and consumer ethics). Technical constraints, as calculated by the GTAP 8 dataset, are emulated in the null model. Social constraints, on the other hand, are randomized entirely.

To begin, we define the regional technical coefficients $\hat{C}_{i,sj}$ and global technical coefficients $\tilde{C}_{i,j}$ to be:

$$\hat{C}_{i,sj} = \frac{\sum_r Z_{ri,sj}}{\sum_{r,i} Z_{ri,sj}}$$

$$\tilde{C}_{i,j} = \frac{\sum_{r,s} Z_{ri,sj}}{\sum_{r,i,s} Z_{ri,sj}} \ .$$

The first characterizes the input requirements of regional industries relative to other industries. Note that the social choice of from which regions to acquire inputs is not described by this matrix. The second $\tilde{C}_{i,j}$ averages these industrial requirements over the entire globe.

Our null model is then constructed as follows:

1. The global technical coefficients $\tilde{C}_{ij}^{(\text{GTAP})}$ from GTAP 8 are used as a baseline to generate regional technical coefficients. Namely, for each region r and industry j the technical coefficients $\hat{C}_{i,rj}$ are drawn as:

$$\hat{C}_{i,rj} \sim \text{Dir}\left(\alpha_i = \zeta_{C,i}\hat{C}_{i,rj}\right) .$$

This ensures that the technical composition of local industries is similar to that found in the GTAP 8 database. The vector parameter $\zeta_{C,i}$ controls the degree of similarity.

2. The regional spending distribution $s_{a,r}$, consumption coefficients $c_{i,ra}$, import coefficients $M_{i,sj}$, regional supply coefficients $R_{r,si}$, value-added coefficients U_{ri}, and factor coefficients $F_{u,ri}$ are all drawn from uniform Dirichlets:

$$\begin{aligned}
s_{a,r} &\sim \text{Dir}\left(\alpha_a = 1\right) \\
c_{i,ra} &\sim \text{Dir}\left(\alpha_i = 1\right) \\
(M_{i,sj}, 1 - M_{i,sj}) &\sim \text{Dir}\left(\alpha_1 = 1, \alpha_2 = 1\right) \\
R_{r,si} &\sim \text{Dir}\left(\alpha_r = 1\right) \\
(U_{ri}, 1 - U_{ri}) &\sim \text{Dir}\left(\alpha_1 = 1, \alpha_2 = 1\right) \\
F_{u,ri} &\sim \text{Dir}\left(\alpha_u = 1\right)
\end{aligned} \tag{S1}$$

In order, these describe: the distribution of regional spending among the final demand sectors; the distribution of spending by each final demand sector among its products of consumption; the proportion by which a given industrial sector will import a particular input instead of source it domestically; the regional probability of importing an input from another specific region; the proportion of capital outlay towards factors by a given industrial sector; and the distribution of that capital among the factors. These describe socially-determined relations between the regions and sectors. These are the relationships we seek to randomize in the null model.

3. The full technical coefficients are constructed as:

$$C_{ri,sj} = \begin{cases} (1 - U_{ri})(1 - M_{i,sj})\hat{C}_{i,sj} & r = s \\ (1 - U_{ri})R_{r,si}M_{i,sj}\hat{C}_{i,sj} & r \neq s \end{cases} .$$

From these we define the matrix:

$$K_{r,s} := \sum_{i,j,a} U_{ri} \left(\mathbf{I} - \mathbf{C}\right)^{-1}_{ri,sj} c_{j,sa}s_{a,s} .$$

This matrix describes the likelihood that money originating in a final demand sector in region s ends up in a value-added sector in region r. Now, given any particular global spending distribution $\hat{\mathbf{x}}$, the regional incomes are determined by $\hat{\mathbf{y}} = \mathbf{K}\hat{\mathbf{x}}$. We calculate the eigenvector $\boldsymbol{\pi}$ such that $\mathbf{K}\boldsymbol{\pi} = \boldsymbol{\pi}$. (Its existence is guaranteed by the fact that $\mathbf{L}$ is stochastic in its left index.) If spending matched this eigenvector, then no region would hold a trade deficit or surplus. All trade would be equally balanced. The spending in our model is drawn from a Dirichlet as:

$$\hat{x}_r \sim \text{Dir}(\alpha_r = \zeta_X \pi_r) .$$

Thus, the parameter ζ_X controls the scale of trade imbalance.

4. The multiregional input-output table can now be constructed as:

$$D_{ri,ra} = c_{i,ra}s_{a,r}\hat{x}_r$$

$$Z_{ri,sj} = \sum_{\substack{t\in\mathcal{R}\\k\in\mathcal{I}_0\\a\in\mathcal{D}_0}} C_{ri,sj}\left(\mathbf{I}-\mathbf{C}\right)^{-1}_{sj,tk}D_{tk,ta} \qquad (S2)$$

$$V_{ru,ri} = \sum_{\substack{s\in\mathcal{R}\\j\in\mathcal{I}_0\\a\in\mathcal{D}_0}} F_{u,ri}U_{ri}\left(\mathbf{I}-\mathbf{C}\right)^{-1}_{ri,sj}D_{sj,sa}$$

From $Z_{ri,sj}$ we compute the sector activities $z_{ri}=\sum_{s,j}Z_{ri,sj}$ and finally the attribution matrix:

$$A_{ri,sa} = \frac{\left[\left(\mathbf{I}-\mathbf{C}\right)^{-1}\mathbf{D}\right]_{ri,sa}}{z_{ri}} \ .$$

The parameters will be generally set at baseline values $\bar{\zeta}_{C,i}$ and $\bar{\zeta}_X$, determined by:

$$\bar{\zeta}_{C,i}^{-1} = \sum_{\substack{r\in\mathcal{R}\\j\in\mathcal{I}_0}} \frac{v_{ri}^{(\mathrm{GTAP})}}{\sum_s v_{si}^{(\mathrm{GTAP})}}\hat{C}_{j,ri}^{(\mathrm{GTAP})}\log\left(\frac{\hat{C}_{j,ri}^{(\mathrm{GTAP})}}{\bar{C}_{j,i}^{(\mathrm{GTAP})}}\right)$$

$$\bar{\zeta}_X^{-1} = \sum_{r\in\mathcal{R}}\hat{x}_r^{(\mathrm{GTAP})}\log\left(\frac{\hat{x}_r^{(\mathrm{GTAP})}}{\pi_r^{(\mathrm{GTAP})}}\right) \qquad (S3)$$

This uses the Kullback-Liebler divergence [56] as a proxy for the degree of difference between various empirical distributions. This sets the baseline for similar variations within the null model.